Simplified Coherent Synaptic Receptor for Filterless Optical Neural Networks

Bernhard Schrenk, *Member, IEEE*

***Abstract*— Neuromorphic computing is touted to be a game changer for existing and emerging data processing applications. Towards this direction, artificial neural network implementations have moved into the focus of research. Advancing neural networks to the optical domain offers several advantages, such as high data throughput at time-of-flight inference latency. The present work proposes coherent synaptic interconnects as a path towards filterless neural networks with increased routing flexibility. A coherent synaptic receptor with integrated weighing functionality is experimentally investigated and evaluated for a 1-GHz train of 130-ps wide spikes. Homodyne detection is accomplished through use of an optically injection locked local oscillator, while its phase and the responsivity of the co-integrated photodiode are exploited to realize a tunable weight upon reception of the incoming optical spikes. Moreover, the switching of the sign is shown for the detection weight, underpinning the feasibility to extend the allocation of synapses toward both, wavelength and time dimensions.**

***Index Terms*— Optical signal detection, Neural network hardware, Electroabsorption-modulated laser, Neuromorphics**

I. Introduction

IT IS WIDELY recognized that the long-lasting performance increase of traditional computing has flattened out during the past decade as further scaling has been considerably slowed down by the saturation of clock frequency and the von-Neumann bottleneck [1]. As the computing realm is about to experience a performance brick-wall for information processing, a paradigm change in how computing systems are conceived is required in order to retain a continuing growth in computational efficiency. Neuromorphic computing is touted to be a trigger for such, by virtue of its higher processing throughput that goes along with a reduced energy cost [2]. The development of bio-inspired artificial neural networks requires to port the constituent neuromorphic elements such as neurons, the dendritic and axonal arbors within the synaptic interconnects, together with a suitable representation of the respective action potentials, to a technology platform.

Although impressive strides have been made with respect to scaling microelectronic artificial neural networks, their operation is limited to the MHz regime and is further challenged by the high interconnect density for a larger number of neurons.

Photonic circuits suit perfectly in order to serve the synaptic interconnect. On the one hand, it is well known from optical telecommunications that wavelength division multiplexed (WDM) signal transmission can enable a high interconnect density, without the need for massively parallel physical waveguides. On the other hand, several concepts have been proposed to accomplish signal processing. Coherent networks use a single wavelength and phase encoding to perform larger-scale matrix operations in low-loss Mach-Zehnder interferometer mesh structures [3-5]. However, controlling optical phase shifters at high speed beyond the MHz range becomes a challenging exercise. Alternatively, spiking neural networks can mimic the dynamics of biological networks through use of opto-electronic functions with close isomorphism to the biological counterparts. They feature GHz information processing rates, accomplished at high energy efficiency [6]. Multiple wavelengths are typically employed in these network implementations to support scalability of vector multiply-accumulate (MAC) operations [7, 8]. In order to reap the performance benefits of GHz operation at ultra-low time-of-flight latency, the aspects of signal transformation need to be accomplished at the optical domain as well. First steps towards all-optical neural networks have been made through proving the non-linear activation of neurons at the optical domain [6, 9] or through hybrid opto-electronic schemes [10-12]. Further implementation schemes for neuromorphic circuits have been proposed on free-space diffractive optics [13, 14] or superconducting platforms [15].

Application-wise, critical tasks such as predictive control or pattern classification have been demonstrated through neural networks featuring 24 and 11 neural nodes, respectively [10, 11]. Such small-scale photonic neural networks, which build on the principles of artificial intelligence in order to solve time-critical tasks, can be seen as a first application field in the domain of neuromorphic computing.

Experimentally demonstrated MAC functions of recent works that are targeting GHz information rates are mostly based on weighted addition through dedicated photonic elements, followed by a photodetector as the synaptic receptor. Weighing has been proposed by exploiting the excess loss of detuned micro-ring filters in combination with spectral multiplexing through the same resonant structures [9,

Manuscript received June 1, 2021. This work was supported in part by funding from the European Union's Horizon 2020 research and innovation programme through the European Research Council (ERC) under grant agreement No 804769.

Bernhard Schrenk is with the AIT Austrian Institute of Technology, Center for Digital Safety&Security, Giefinggasse 4, 1210 Vienna, Austria (phone: +43 50550-4131; fax: -4150; e-mail: bernhard.schrenk@ait.ac.at).

This article has been accepted for publication in IEEE Journal of Selected Topics in Quantum Electronics. This is the author's version which has not been fully edited and content may change prior to final publication. Citation information: DOI 10.1109/JSTQE.2021.3108573

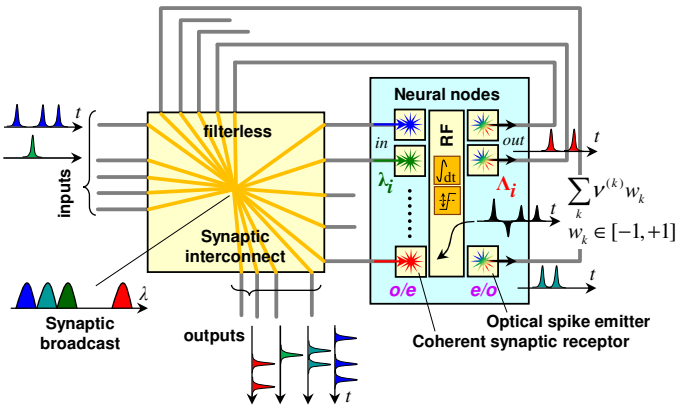

Fig. 1. Hybrid opto-electronic coherent optical neural network architecture. Optical inputs to the neural network and spiking emitters of upstream neurons jointly feed the downstream synaptic receptors and the neural network outputs in a WDM-enabled broadcast-and-select architecture.

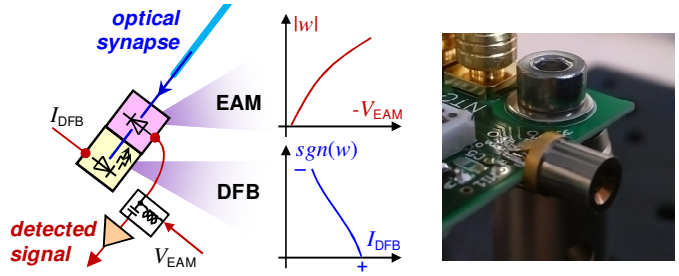

Fig. 2. Principal scheme of the synaptic coherent receptor. Homodyne detection builds on a DFB-based LO that is injection-locked by the optical synapse and a preceding EAM photodiode. Tuning of the detection weight w in terms of magnitude and sign is accomplished through electrical setting of the EAM photodiode responsivity as function of the EAM bias V_{EAM} and the LO phase as function of the DFB bias I_{DFB}, respectively.

16], per-channel gain tuning through active amplifier elements and passive combination of WDM ensembles [11], or self-homodyne detection of inphase/quadrature modulated branches, which additionally allows to choose the sign of the weight [17]. Similarly, self-homodyne detection can be applied through amplitude/phase weighing of local oscillator pulses [18]. These self-homodyne approaches demonstrate a path towards coherent networks at GHz rates.

Likewise, this work aims at a coherent neuromorphic implementation and integrates MAC functionality with the synaptic optical receptor for hybrid opto-electronic neurons, without resorting to additional photonic elements. It extends an initial experimental study [19] by characterizing and demonstrating synaptic weighing in magnitude and sign through a single-ended coherent receiver, taking advantage of homodyne detection with phase-tunable local oscillator (LO). The simplified coherent synaptic receptor is inspired by an electro-absorption modulated laser (EML) and will be operated at a 1-GHz train of 130-ps wide spikes. Moreover, burst-wise sign switching will be shown for the weighted synaptic reception.

The paper is organized as follows. Section II introduces the concept of a coherent synaptic interconnect and highlights the enabling synaptic receptor. Section III characterizes the involved opto-electronic receiver. Section IV discusses the performance for transmission of a spike train and the constraints for scaling up a neural network, while Section V investigates switching of the detection weight during reception. Finally, Section VI concludes the work.

II. Towards Coherent-Optical Neural Networks

A. *Filter- and directionless synaptic interconnect*

The proposed optical neural network architecture leverages coherent reception in a way to enable a passive split for its synaptic interconnect between upstream- and downstream neurons. Figure 1 presents this neural fabric. Optical input signals to the neural network and the optical outputs of neurons are broadcasted at different wavelengths to the inputs of downstream neurons and the outputs of the neural networks. A passive star coupler accomplishes the signal distribution in this broadcast-and-select WDM architecture, which becomes filterless, provided that the synaptic receptors can facilitate the selection of a WDM channel (i.e. synapse) by means of coherent detection. The spike emitters are de-coupled from the synaptic receptors through opto-electronic signal conversion at the neural nodes. As a result, the synaptic receptor and the spike emitter operate at different wavelength channels λ_i and Λ_i, respectively. Wavelength channels can further be subject to a tempo-spectral mapping, where the wavelength is time-shared among multiple, independent signals. In this way, a number of upstream spike emitters can feed a single downstream synaptic receptor.

In order to compose a deep neural network consisting of multiple layers of neurons [1], neural nodes that belong to subsequent layers within a network can be spectrally mapped together. This is accomplished by matching the optical frequencies of upstream spike emitters to those of downstream synaptic receptors. Since every neuron can serve every neural network layer by virtue of its colorless behavior, a flexible allocation of neurons – available as hardware resource – to various layers of the neural network – established as virtual point-to-point links – is possible. At the same time, recurrent neural network architectures can be in principle supported, meaning that the emitter of a neural node can feed back to the synaptic receptor of the same node according to some defined temporal mapping.

It shall be noted that the scalability of the (tempo-)spectral mapping and the synthesis of deep neural networks is not the main scope of the present work, which rather focuses on the enabling synaptic receptor. The adoption of coherent signal transmission in the context of a filterless, ultra-dense WDM signal distribution is highly attractive. First, it provides the ability to select a channel in a broadcast-and-select fashion, which is accomplished through the coherent detection process and thus without extra optical filter element. Second, its higher reception sensitivity allows for a higher optical budget between spike emitter and synaptic receptor. Both together permit an any-to-any architecture with a potentially high fan-in and a high fan-out at both, dendritic and axonal arbors. However, the introduction of coherent detection in optical

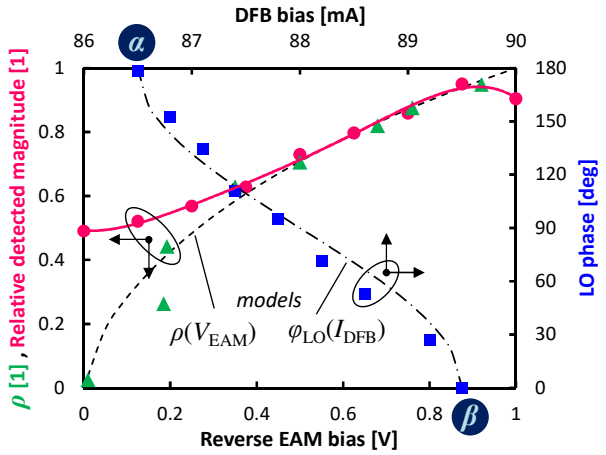

Fig. 3. Model and experimental characterization of the accomplished weighing process through the EML receiver.

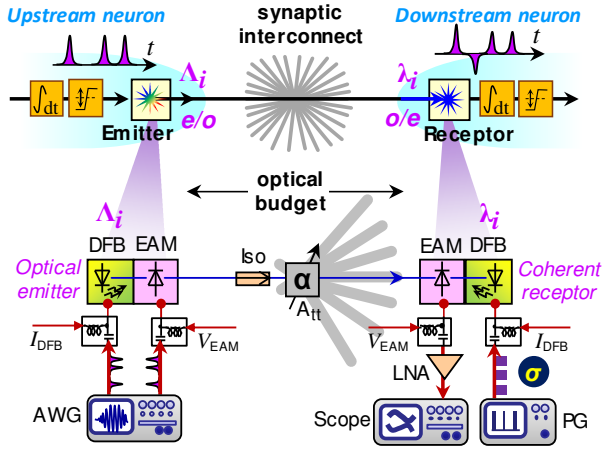

Fig. 4. Coherent pipe over the synaptic interconnect and corresponding experimental setup.

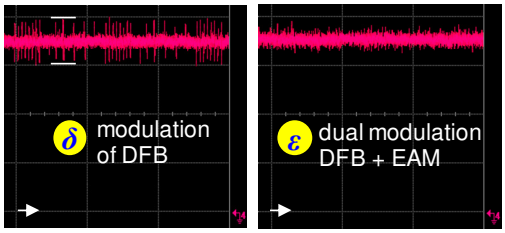

Fig. 5. Optical output signal of the phase-coded optical spike emitter.

neural networks comes at a major technical challenge: the realization of a simplified coherent synaptic receiver. This work will investigate whether MAC functionality can be partially integrated with the synaptic receptor, in terms of including the weighing process with respect to both, magnitude and sign.

B. Coherent synaptic receptor

The prerequisite for a simplified coherent receptor necessitates the omission of digital signal processing (DSP) after the detection process, such as typically employed for the purpose of frequency offset estimation and carrier-phase recovery. Analogue homodyne reception is therefore seen as the prime implementation option. Figure 2 illustrates the concept for the synaptic receptor, which is inspired by an EML. It builds on three key notions: First, homodyne reception is supported through optical injection locking [20] of the LO. In case of the EML-inspired receptor, this means that the incident synapse locks the distributed feedback (DFB) laser of the EML all-optically, which is considered to be simpler than alternative approaches such as phase-locked loops [21, 22]. The mechanism of injection locking will be characterized in Section III. As will be discussed shortly in more detail, the coherent receptor is completed through the electro-absorption modulator (EAM) based photodiode, at which the incident optical synapse and the LO beat. Since there is no optical frequency difference between the two optical fields, the information associated to the synapse is down-converted to the electrical baseband without frequency offset, while a stable phase between the LO and the optical input to the receptor mitigates phase noise otherwise present in the received electrical signal.

The direct-detection and coherent-detection terms of the photocurrent I_{EAM} after single-ended opto-electronic down-conversion of the incident optical signal P_{syn} are given by [23]

$$i_{EAM}(t) = R(V_{EAM})\Big[P_{syn}(t) + P_{LO} + 2\sqrt{P_{syn}(t)P_{LO}}\cos\left(\omega_{IF}t + \varphi_{syn} - \varphi_{LO}\right)\Big] \quad (1)$$

where R is the bias-dependent responsivity of the EAM photodiode, P_{LO} the optical power of the DFB-based LO, ω_{IF} relates to the intermediate frequency after down-conversion, and φ_{syn} and φ_{LO} denotes the optical phase of the incident signal and the LO, respectively. By beating the LO and the optical input at the EAM, coherent homodyne detection is accomplished, and a vanishing residual frequency offset and a stable phase are yielded so that $\omega_{\mathrm{IF}} = 0$. As a consequence, DSP-free reception can be accomplished.

The second notion is the responsivity tuning of the EAM photodiode through its bias voltage V_{EAM}, which contributes the magnitude of the weight for the incident synapse. The responsivity depends on the detection function ρ of the EAM,

$$R(V_{\mathrm{EAM}}) = R_0\,\rho(V_{\mathrm{EAM}}) \quad (2)$$

whereas the function ρ is yielded through

$$\rho(V_{\mathrm{EAM}}) = 1 - \tau(V_{\mathrm{EAM}}) \quad (3)$$

with R_0 being a normalization factor and τ being the transmission of the EAM, given by [24]

$$\tau(V_{EAM}) = T_0\left(1-\varepsilon_{\min}\right)\exp\left[-\left(\frac{V_{EAM}}{V_a}\right)^{\alpha}\right] + \varepsilon_{\min} \quad (4)$$

where V_{a} and α are fitting parameters, T_0 accounts for intrinsic losses and $\varepsilon_{\min}$ is the minimum extinction. A typical function ρ is plotted in Fig. 3 for V_a = -2V, α = 0.65 and $\varepsilon_{\min}$ = 0.01. As such, the EAM can be used to determine the

This article has been accepted for publication in IEEE Journal of Selected Topics in Quantum Electronics. This is the author's version which has not been fully edited and content may change prior to final publication. Citation information: DOI 10.1109/JSTQE.2021.3108573

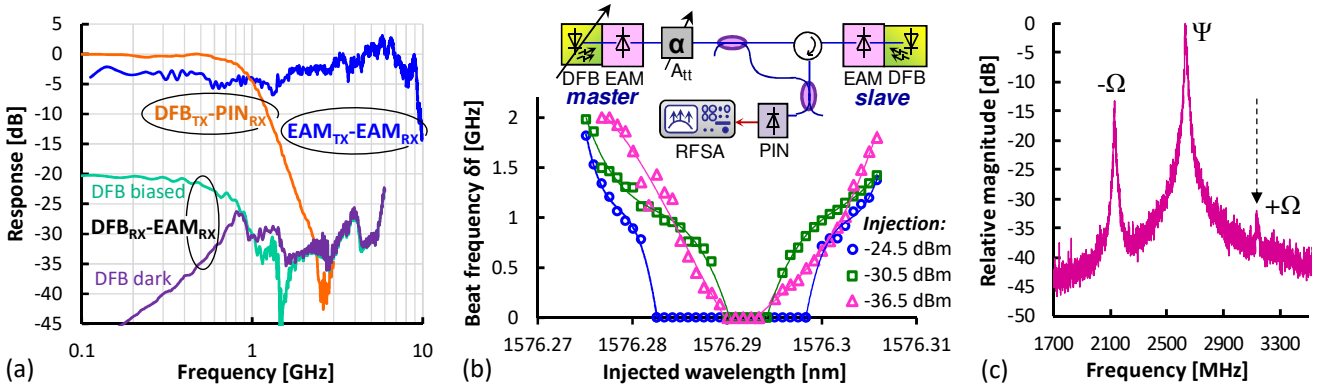

Fig. 6. (a) Electro-optic and end-to-end responses for EML sections. (b) Injection locking range. (c) Pilot tone spectrum for weight calibration.

magnitude of the weight with which the input synapse is acquired.

Third, the LO phase φ_{LO} can be determined by the DFB bias current I_{DFB} within a π-phase range and is determined by [25]

$$\varphi_{LO} - \varphi_{syn} = -\arcsin\left(\frac{\Delta\nu}{\delta\nu_{LR}}\right) - \arctan\alpha \tag{5}$$

where $\delta\nu_{LR}$ is the half-width locking range of the LO and α is the linewidth enhancement factor. The frequency offset $\Delta\nu$ between the optical input signal and the LO at its native (corresponding to the free-running) and DFB bias dependent emission frequency is

$$\Delta\nu = \nu_{syn} - \nu_{LO}(I_{DFB}) \tag{6}$$

This mechanism for tuning the LO phase therefore alters the sign of the weight since the phase of the LO determines the sign of the coherent detection term of the EAM photocurrent, as it is evidenced through the respective term in Eq. (1).

With the control of EAM and DFB, excitatory and inhibitory synapses can be facilitated without resorting to a dual-port optical element such as a ring resonator [16] or a balanced detector [18]. Moreover, the use of an EML as a multi-functional opto-electronic element [26] for both, spike emission and "signed" coherent homodyne detection, contributes to a flexible neural fabric. This is because EML elements can be allocated on-demand in order to the address the need for receptor and emitter functions that are required for the actual network synthesis.

III. Experimental Characterization

The coherent-optical synaptic interconnect and the corresponding synaptic receptor have been evaluated in the experimental setup shown in Fig. 4. The arrangement resembles a virtual point-to-point branch of an interconnect and includes an optical spike generator at the transmitter side, and the receptor with integrated optical weighing function at the receiver side. Although the signal representation for the spikes traversing the synaptic interconnect can be based on multiple formats, the present work chooses a phase format when converting the electrical spikes to the optical domain, and vice versa.

As proposed, EMLs have been employed at the spike emitter and the synaptic receptor. Transistor-outline (TO) EMLs operating at 1577 nm have been used in particular (see inset in Fig. 2). These feature an integrated micro-cooler, which is required for coarse spectral alignment. In a fully integrated optical neural network, this cooler is believed to be obsolete since both end-points of the synaptic interconnect are hosted on the same, chip-scale neuromorphic platform. This argument is underpinned by the fact that the two, independent EMLs in this work were featuring a small frequency offset of just 1.7 GHz between their optical emission frequencies of 190.1 THz when being operated at the same DFB bias current and temperature. This offset can be eliminated through DFB bias current tuning, which typically shifts the optical LO frequency by 0.54 GHz/mA into a locked condition.

The optical spike emitter builds on chirp modulation of its DFB section in order to accomplish a π-phase shift at its output [27], using a pulse-reformatted drive signal. This direct laser modulation is accompanied by unwanted amplitude modulation, which leads to an intensity modulation extinction ratio of 1.13 dB. In order to revert to a constant-intensity signal, the EAM section is synchronously modulated by the inverse DFB drive with adjusted swing. The resulting intensity signature of the EML output showed a reduced extinction ratio of 0.45 dB. Figure 5 reports the output signal of the spike emitter without (δ) and with (ε) EAM modulation, respectively. Figure 6(a) presents the electro-optic modulation response of the DFB section, which was acquired using a 10-GHz PIN photoreceiver as detector. The -3-dB bandwidth of the DFB section was 0.91 GHz under typical bias conditions, while it was 7.3 GHz for the EAM section.

A variable optical attenuator (A_{tt}) connects the optical emitter to the synaptic receptor. Two more auxiliary items have been added to the interconnect, in order to ensure optimal operation in a fiber-based synaptic interconnect. First, polarization alignment of the delivered optical signal with the receptor is accomplished through manual polarization control. However, there is no need for polarization drift compensation for chip-scale artificial neural networks. Second, and optical isolator has been added in order to eliminate optical phase fluctuations along the fiber-based link that would worsen the bidirectional locking stability among the two EMLs. A stable

This article has been accepted for publication in IEEE Journal of Selected Topics in Quantum Electronics. This is the author's version which has not been fully edited and content may change prior to final publication. Citation information: DOI 10.1109/JSTQE.2021.3108573

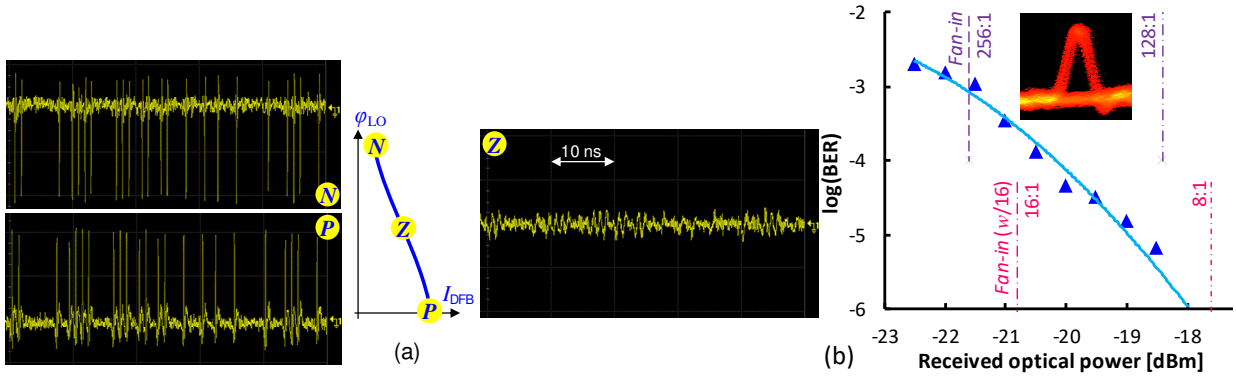

Fig. 7. (a) Detected spike trains for various LO phase settings and (b) corresponding BER performance for the received spike train with positive sign.

directionless and non-isolated EML-to-EML link has been experimentally demonstrated earlier in a free-space communication arrangement [28], which resembles the conditions of chip-integrated links more closely than a fiber-based lightpath.

The synaptic coherent receptor is injection-locked to the optical input signal through adjusting any of the DFB bias currents, either at the optical emitter or the receptor. The injection locking process has been characterized in terms of locking range and corresponding experimental results are presented in Fig. 6(b). The emission of two EMLs is beating at a PIN receiver and the beat note frequency δf is acquired through a RF spectrum analyzer (RFSA). One of the EMLs serves as master and delivers an optical feed to the slave EML. Under injection locking, the emission frequency of the slave EML is synchronized to that of the master so that δf = 0. This spectral region has been determined by detuning the master EML wavelength and is plotted in Fig. 6(b). The injection locking range is 2.1 and 0.6 GHz at an injection power of -24.5 and -36.5 dBm, respectively. Moreover, the DFB current tuning range that covers this spectral band for the EML emission frequency, at which the slave EML locks to its master, is a few mA wide and thus sufficiently large to allow a precise setting for the tuning of the LO with state-of-the-art current controllers.

At the same time, the detection weight is selected through the EAM and DFB biases, as will be discussed shortly. The detected photocurrent of the EAM, for which a typical bias is in the range of -0.75V, is post-amplified by a 50Ω low-noise amplifiers (LNA). The end-to-end response over the EAM-to-EAM link is appended to Fig. 6(a). It proves that high frequencies up to 10 GHz can be supported through the TO-can EML tandem. Higher bandwidths are believed to be accessible through wire-bonding of die-level components for the opto-electronic converter and the electronic front-end.

In order to calibrate the weight that is applied for the reception within the coherent pipe between optical emitter and receptor, a pilot tone has been modulated on the optical carrier. Single-sideband modulation is performed in order to avoid fading effects of the detected tone after injection-locked homodyne detection at the receptor. It is accomplished through dual-modulation of DFB and EAM sections at the optical emitters with phase- and swing-adjusted setting for the respective electrical sinusoidal driving signals. Figure 6(c) presents the pilot tone spectrum for a tone at Ω = 500 MHz. It has been acquired through heterodyned detection with the synaptic receptor, for which the LO has been purposely detuned to shift the optical carrier to an intermediate frequency of Ψ = 2.63 GHz for the detected signal. The suppression of the mirror frequency at +Ω with respect to the tone at -Ω relative to the intermediate frequency Ψ is 18.8 dB. In order to perform the calibration, the received optical tone is compared to a local replica of the electrical tone and the relative phase shift is acquired within the locking range through fine tuning of the DFB bias current I_{DFB}. The result of this characterization is appended to the LO phase in Fig. 3 (■). The experimental data agrees well with the model and confirms that the sign of the detected signal can be alternated.

Moreover, the responsivity of the EAM detector has been tuned through adjustment of its bias V_{EAM}. The reduction in magnitude for the detected signal is also introduced to Fig. 3 (●), together with the experimental data for the bias-dependent EAM transmission τ, expressed as detection function ρ (▲) according to Eq. (3). Model and experiment agree for medium and large EAM bias V_{EAM}, but deviate from the model for low bias voltages. In this region, a lower weight magnitude could be obtained by exploiting phase orthogonality between incident signal and LO, as will be proven in the Section IV. Such a condition can be accomplished through LO phase adjustment, as it is exclusively used for sign switching at present.

IV. Reception of a Spike Train and Scalability

In order to evaluate the performance of the coherent synaptic interconnect link, the optical emitter was sourced by a pseudo-random bit sequence (PRBS) with a rate of 1 GHz and a spike width of 130 ps. Figure 7(a) presents the same spike train for the two settings of the sign, positive (P) and negative (N), which are chosen through LO phase tuning toward the two boundaries of the locking range and which are shown for the maximum magnitude of the detection weight. The clearly distinguishable spikes adhere to the PRBS pattern, which confirms that the EML-inspired receptor accomplishes coherent homodyne detection in absence of DSP.

It is further possible to quench the received spike train entirely through adjusting the LO phase orthogonal to that of

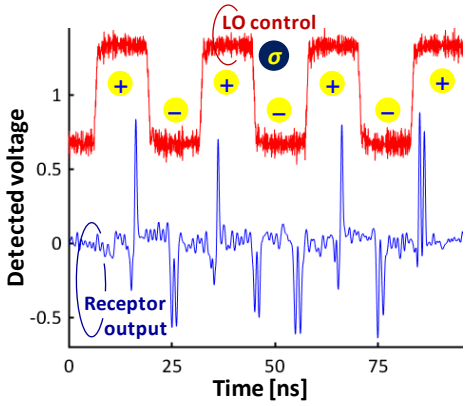

Fig. 8. Sign switching of the detected signal through LO phase modulation.

the incident optical signal. This case is shown in Fig. 7(a) as Z, for which only the residual intensity modulation artifacts of the transmitted signal remain.

The bit error ratio (BER) has been acquired as function of the received optical power through acquisition of the spike train with a real-time oscilloscope and sub-sequent error counting. Figure 7(b) reports the BER performance for the spike train with positive sign setting. A reception sensitivity of -20.7 dBm is obtained at a BER of 2.10^{-4}. This equates to an optical budget of more than 24 dB, given the optical launch of 4 dB from the optical emitter. The budget corresponds to a 128:1 fan-in over a passive distribution split, which by virtue of coherent reception bears the potential to be filterless.

However, the optical budget is not to be exclusively dedicated to the fan-in/out loss of the synaptic interconnect. Given the requirement of weighing synapses over a resolution of, e.g., 4 bit, an extra loss of 12 dB would apply in case the weighing process is perceived as an optical loss factor. Under this worst-case weight, the compatible loss budget would permit a 16:1 fan-in (Fig. 7(b), see *w*/16). Under the introductorily motivated application settings of ~25 neurons for a neural network, this fan-in would be too low in view of the endeavored broadcast-and-select architecture and its filterless synaptic interconnect. However, further improvement of the optical budget in the order of ~10 dB is expected by replacing the LNA used in this work with a transimpedance amplifier, which is to be closely co-integration with a die-level rather than a TO-can EML device.

Another aspect that is to be addressed when scaling up a coherent optical neural network is the tunability of the involved light sources. In the present experiment, a DFB-assisted source and LO have been adopted at the spike emitter and synaptic receptor, respectively. Considering the typical tuning range of -1 / +2 nm of the DFB laser and the homodyne detection of narrowly spaced synaptic signals with 130 ps spike width, the number of synaptic signals in the broadcast-and-select architecture is limited to only 18 channels. It is therefore paramount to adopt optical source schemes with wider tunability, such as distributed Bragg reflector (DBR) assisted designs or alternative tunable laser schemes.

V. Time-Switched Signed Coherent Reception

The small duty cycle of the optical spikes motivates the extension from a purely spectral to a hybrid tempo-spectral allocation of synapses. This migration from the WDM domain, which is accomplished through incorporation of time division multiplexing (TDM), similar as proposed in [18], facilitates multiple inputs per synaptic receptor of a neural node. The weighted inputs can then be accumulated by the receptor through integration at the electrical domain, within a period of the TDM frame.

One key requirement to form a weighted sum of inputs is the alteration of the weight during the reception of a spike train. In a first evaluation towards this direction, the sign of the detection weight has been flipped. A pulse generator (PG) has been employed to periodically switch the LO phase (σ in Fig. 4) at a frequency of 40 MHz.

However, crosstalk arises from the modulated DFB-section of the LO to the EAM photodiode. The crosstalk magnitude is characterized through the transmission function between the respective sections of the receiving EML, as shown in Fig. 6(a). The S21-parameter between DFB and EAM sections at the receiver shows a non-negligible response for the lit DFB with a peak value of around -20 dB, while for the dark DFB the crosstalk drops. This means that crosstalk arises from the intensity modulation of the LO emission rather than through insufficient isolation between the DFB and EAM sections. The mitigation of this modulation crosstalk requires a feed-forward cancellation of the LO control signal. For the sake of simplicity, this cancellation was implemented in the digital domain after time-synchronized acquisition of the LO control next to the detected signal; However, this cancellation can be performed in the analogue radio frequency domain, as it is for example known from feed-forward cancellation schemes in full-duplex optical access networks with wavelength-reuse [29].

Figure 8 presents the detected spike trace after crosstalk mitigation, together with the control signal of the LO (σ). Depending on the disciplined polarity, the spikes at the receiver output are signed either positively or negatively. This proves the principal suitability of the proposed receiver to change the weight parameters for time-slotted synaptic reception. Further study is required towards a faster weight modulation in both, sign and magnitude.

VI. Conclusion

A coherent optical synaptic interconnect concept has been proposed and the synaptic receptor as the key enabling component has been experimentally evaluated. Towards this direction, a low-complexity, EML-inspired homodyne detector has been demonstrated to integrate weighing functionality through responsivity and LO phase tuning. Reception of a 1-GHz spike train with 130-ps spike width has been accomplished. Moreover, the possibility for time-switching of the detection weight for an advancement to a hybrid WDM/TDM allocation of synapses at the neural interconnect has been investigated. The wavelength-selective detection in a

neural fabric bears the potential to realize a filterless synaptic interconnect. Higher fan-in ratios are expected for receptors that benefit from transimpedance amplifier based reception, which in the present work were not accessible due to a packaged EML chip. Photonic circuit integration of a non-isolated synaptic link between spike emitter and receptor is left for future work.

ACKNOWLEDGMENT

The author would like to thank Margareta Stephanie for her support during the experimental characterization of the receptor device.

REFERENCES

[1] J.D. Kendall, and S. Kumar, "The building blocks of a brain-inspired computer," *Appl. Phys. Rev.*, vol. 7, no. 1, p. 011305, Jan. 2020.
[2] J. Hasler, and B. Marr, "Finding a roadmap to achieve large neuromorphic hardware systems," *Front. Neurosci.*, vol. 7, p. 118, Sep. 2013.
[3] N. Harris *et al.*, "Linear programmable nanophotonic processors," *Optica*, vol. 5, no. 12, pp. 1623-1630, Dec. 2018.
[4] F. Shokraneh, S. Geoffroy-Gagnon, M.S. Nezami, and O. Liboiron-Ladouceur , "A Single Layer Neural Network Implemented by a 4 × 4 MZI-Based Optical Processor," *Phot. J.*, vol. 11, no. 6, p. 4501612, Dec. 2019.
[5] H. Zhang *et al.*, "An optical neural chip for implementing complex-valued neural network," *Nature Comm.*, vol. 12, p. 457, 2021.
[6] P.R. Prucnal, B.J. Shastri, T. Ferreira de Lima, M.A. Nahmias, and A.N. Tait, "Recent progress in semiconductor excitable lasers for photonic spike processing," *Advances in Optics and Phot.*, vol. 8, no. 2, pp. 228-299, Jun. 2016.
[7] A. Tait, M. Nahmias, B. Shastri, and P. Prucnal, "Broadcast and Weight: An Integrated Network For Scalable Photonic Spike Processing," *J. Lightwave Technol.*, vol. 32, no. 21, pp. 4029-4041, Nov. 2014.
[8] J. Feldmann *et al.*, "Parallel convolutional processing using an integrated photonic tensor core," *Nature*, vol. 589, pp. 52-58, 2021.
[9] J. Feldmann, N. Youngblood, C. Wright, H. Bhaskaran, and W. Pernice, "All-optical spiking neurosynaptic networks with self-learning capabilities," *Nature*, vol. 569, pp. 208-214, 2019.
[10] T. Ferreira de Lima *et al.*, "Machine Learning With Neuromorphic Photonics," *J. Lightwave Technol.*, vol. 37, no. 5, pp. 1515-1534, Mar. 2019.
[11] B. Shi, N. Calabretta, and R. Stabile, "Deep Neural Network Through an InP SOA-Based Photonic Integrated Circuit," *J. Sel. Topics in Quantum Electron.*, vol. 26, no. 1, p. 7701111, Jan. 2020.
[12] J. Robertson, M. Hejda, J. Bueno, and A. Hurtado, "Ultrafast optical integration and pattern classification for neuromorphic photonics based on spiking VCSEL neurons," *Sci. Rep.*, vol. 10, p. 6098, Apr. 2020.
[13] J. Bueno *et al.*, "Reinforcement learning in a large-scale photonic recurrent neural network," *Optica*, vol. 5, no. 6, pp. 756-760, 2018.
[14] T. Zhou *et al.*, "Large-scale neuromorphic optoelectronic computing with a reconfigurable diffractive processing unit," *Nature Phot.*, vol. 15, pp. 367-373, 2021.
[15] J. Shainline, S. Buckley, R. Mirin, and S.W. Nam, "Superconducting Optoelectronic Circuits for Neuromorphic Computing," *Phys. Rev. Appl.*, vol. 7, p. 034013, Mar. 2017.
[16] A.N. Tait, J.Chang, B.J. Shastri, M.A. Nahmias, and P.R. Prucnal, "Demonstration of WDM weighted addition for principal component analysis," *Opt. Expr.*, vol. 23, no. 10, pp. 12758-12765, May 2015.
[17] G. Mourgias-Alexandris *et al.*, "Neuromorphic Photonics With Coherent Linear Neurons Using Dual-IQ Modulation Cells," *J. Lightwave Technol.*, vol. 38, no. 4, pp. 811-819, Feb. 2020.
[18] R. Hamerly, L. Bernstein, A. Sludds, M. Soljacic, and D. Englund, "Large-Scale Optical Neural Networks Based on Photoelectric Multiplication," *Phys. Rev. X*, vol. 9, p. 021032, May 2019.
[19] B. Schrenk, "Coherent Homodyne Synaptic Interconnect with Sign- and Weight-Tunable Detection," in *Proc. Opt. Fib. Comm. Conf.*, San Francisco, United States, Jun. 2021, paper Tu5H.7.
[20] B. Schrenk, "Injection-Locked Coherent Reception Through Externally Modulated Laser," *J. Sel. Topics in Quantum Electron.*, vol. 24, no. 2, p. 3900207, Mar. 2018.
[21] T. Hirokawa *et al.*, "Analog Coherent Detection for Energy Efficient Intra-Data Center Links at 200 Gbps per Wavelength," *J. Lightwave Technol.*, vol. 39, no. 2, pp. 520-531, Jan. 2021.
[22] K. Balakier, L. Ponnampalam, M.J. Fice, C.C. Renaud, and A.J. Seeds, "Integrated Semiconductor Laser Optical Phase Lock Loops," *J. Sel. Topics in Quantum Electron.*, vol. 24, no. 1, p. 1500112, Jan. 2018.
[23] K. Kikuchi, "Fundamentals of Coherent Optical Fiber Communications," *J. Lightwave Technol.*, vol. 34, no. 1, pp. 157-179, Jan. 2016.
[24] R.A. Salvatore, R.T. Sahara, M.A. Bock, and I. Libenzon, "Electroabsorption Modulated Laser for Long Transmission Spans," *J. Quantum Electron.*, vol. 38, no. 5, pp. 464-476, May 2002.
[25] F. Mogensen H. Olesen, and G. Jacobsen, "Locking Conditions and Stability Properties for Semiconductor Laser with External Light Injection," *J. Quantum Electron.*, vol. 21, no. 7, pp. 784-793, Jul. 1985.
[26] B. Schrenk, "The Electroabsorption-Modulated Laser as Optical Transmitter and Receiver: Status and Opportunities", *IET Optoel.*, vol. 14, pp. 374-385, 2020.
[27] J.A. Altabas, D. Izquierdo, J.A. Lazaro, and I. Garces, "Chirp-based direct phase modulation of VCSELs for cost-effective transceivers," *Opt. Lett.*, vol. 42, no. 3, pp. 583-586, 2017.
[28] B. Schrenk, D. Milovancev, N. Vokic, and F. Karinou, "Face-to-Face EML Transceiver Tandem for Full-Duplex Analogue Radio-over-Air", *J. Lightwave Technol.*, vol. 38, no. 11, pp. 2976-2983, Jun. 2020.
[29] J.H. Yu, N. Kim, and B.W. Kim, "Remodulation schemes with reflective SOA for colorless DWDM PON," J. Opt. Netw., vol. 6, no. 8, pp. 1041-1054, Aug. 2007.

Bernhard Schrenk (S'10-M'11) was born 1982 in Austria and received the M.Sc. ('07) degree in microelectronics from the Technical University of Vienna. He was at the Institute of Experimental Physics of Prof. A. Zeilinger, where he was involved in the realization of a first commercial prototype for a quantum cryptography system, within the European SECOQC project. From 2007 to early 2011 he obtained his Ph.D degree at UPC BarcelonaTech, Spain. His Ph.D thesis on multi-functional optical network units for next-generation Fiber-to-the-Home access networks was carried out within the FP7 SARDANA and EURO-FOS projects. In 2011 he joined the Photonic Communications Research Laboratory at NTUA, Athens, as post-doctoral researcher and established his research activities on coherent FTTH under the umbrella of the FP7 GALACTICO project. In 2013 he established his own research force on photonic communications at AIT Austrian Institute of Technology, Vienna, where he is working towards next-generation metro-access-5G networks, photonics integration technologies and quantum optics. Dr. Schrenk has authored and co-authored ~180 publications in top-of-the-line (IEEE, OSA) journals and presentations in the most prestigious and highly competitive optical fiber technology conferences. He was further awarded with the Photonics21 Student Innovation Award and the Euro-Fos Student Research Award for his PhD thesis, honoring not only his R&D work but also its relevance for the photonics industry. He was elected as Board-of-Stakeholder member of the Photonics21 European Technology Platform in 2017 and is serving as Technical Program Committee member for the ECOC conference. During his extensive research activities he was and is still engaged in several European projects such as SARDANA, BONE, BOOM, APACHE, GALACTICO, EURO-FOS and the Quantum Flagship project UNIQORN. In 2013 he received the European Marie-Curie Integration Grant WARP-5. In 2018 he was awarded by the European Research Council with the ERC Starting Grant COYOTE, which envisions coherent optics everywhere.